Magneto-Optical Imaging Studies of Flux Propagation in Ultra-Pure and Carbon-Doped MgB_2 Thin Films

Zuxin Ye, Qiang Li, Yufeng Hu, A. V. Pogrebnyakov, Y. Cui, X. X. Xi, J. M. Redwing, and Qi Li

***Abstract*—The mixed state in *c*-axis oriented ultra-pure MgB_2 thin films and carbon-doped MgB_2 thin films produced by hybrid physical-chemical vapor deposition was studied using magneto-optical imaging (MOI) technique. In the ultra-pure MgB_2 films, a regular magnetic flux penetration pattern was observed, as expected from the Bean critical state model. This is in striking contrast to earlier MOI observations of MgB_2 films made by pulse laser deposition, where dentritic flux jumps were usually abundant at temperature below 10 K. In our carbon-doped MgB_2 thin films, similar dentritic flux jumps were also observed at low temperature and low applied magnetic field. It is evident that the dendritic flux jumps or stability of the film is strongly influenced by the material parameters of the films, rather than inherent in all MgB_2 thin films.**

***Index Terms*—Flux jump, magneto optical, MgB_2, superconductor.**

I. INTRODUCTION

THE discovery of 39 K superconductivity in MgB_2 [1] revealed the great potential of this material in practical applications. However, thermal instability in the form of flux jumps was reported in thin films, wires, and bulk MgB_2 at low temperature [2]–[7]. Using magneto-optical imaging (MOI), Johanson *et al.* first observed dendritic flux jump patterns in MgB_2 thin films grown by pulsed laser deposition (PLD) [2], [3], which is responsible for the dense oscillations reported earlier in magnetization hysteresis loops of similar samples [5]. Since the thermal instability can strongly influence the performance of a superconductor, one of the critical issues in practical application of MgB_2 thin films is to understand the mechanism controlling this instability and find a way to suppress it by adjusting the material properties. Though this dendritic flux jump was believed to be thermal-magnetic in origin [2], [3], the correlation between this phenomenon and material parameters such as critical temperature T_c, upper critical field H_{c2}, normal state resistivity ρ_n, and critical current density J_c, etc., is still poorly understood.

To explore the mechanism of dendritic flux jump, comparative studies were performed on ultra-pure epitaxial MgB_2 thin films and carbon-doped MgB_2 thin films using MOI technique and conventional magnetization measurement. Dendritic flux jump was observed in the carbon-doped films, while a regular uniform flux penetration pattern predicted by critical state models was observed in the ultra-pure MgB_2 thin films. Combined with the complementary transport and magnetization measurements, this MOI study indicates the strong correlation between the occurrence of dendritic flux jump and the flux flow resistivity of the samples. The influence of the sample size on the flux jump pattern was also investigated using MOI on the carbon-doped MgB_2 films with different sizes.

II. EXPERIMENTAL DETAILS

A. *Ultra-Pure* MgB_2 *Thin Films and Carbon-Doped* MgB_2 *Thin Films*

The MgB_2 thin films used in this study were grown on *c*-cut SiC single crystalline substrates by in-situ hybrid physical-chemical vapor deposition (HYCVD) process. The details of sample synthesis have been described previously [8]. A 330 nm-thick ultra-pure MgB_2 thin film and a 200 nm-thick 12 at.% carbon-doped MgB_2 thin film, both 5 mm × 5 mm in size, were selected for MOI study and magnetization measurement. The superconducting transition temperatures were 41.2 K and 38.4 K for ultra-pure and carbon-doped samples, respectively, determined by resistivity measurements. Both samples had sharp transitions with $\Delta T < 0.5$ K.

B. *MOI Experiment and Magnetization Measurement*

The MOI studies were performed on our low temperature MOI station described elsewhere [4]. A bismuth-doped iron garnet indicator film was placed onto the sample surface, with external magnetic field always applied perpendicular to the film surface. Brightness intensity in the images corresponds to the local flux line density. The superconducting properties were also characterized by magnetization measurement on the same samples in a Quantum Design's SQUID magnetometer. The magnetic hysteresis loops (MHL) were measured at various temperatures under external magnetic fields applied perpendicular to film surface.

Manuscript received October 4, 2004. The work at BNL was supported by the U.S. Department of Energy, Office of Basic Energy Science, under Contract DE-AC-02-98CH10886. The work at Penn State was supported in part by ONR under Grants N00014-00-1-0294 (Xi) and N0014-01-1-0006 (Redwing), and by NSF under Grants DMR-0306746 (Xi and Redwing) and DMR-0405502 (Qi Li).

Z. Ye, Q. Li, and Y. Hu are with Brookhaven National Laboratory, Upton, NY 11973 USA (e-mail: qiangli@bnl.gov).

V. Pogrebnyakov, Y. Cui, X. X. Xi, J. M. Redwing, and Q. Li are with Pennsylvania State University, University Park, PA 16802 USA.

Digital Object Identifier 10.1109/TASC.2005.848850

1051-8223/$20.00

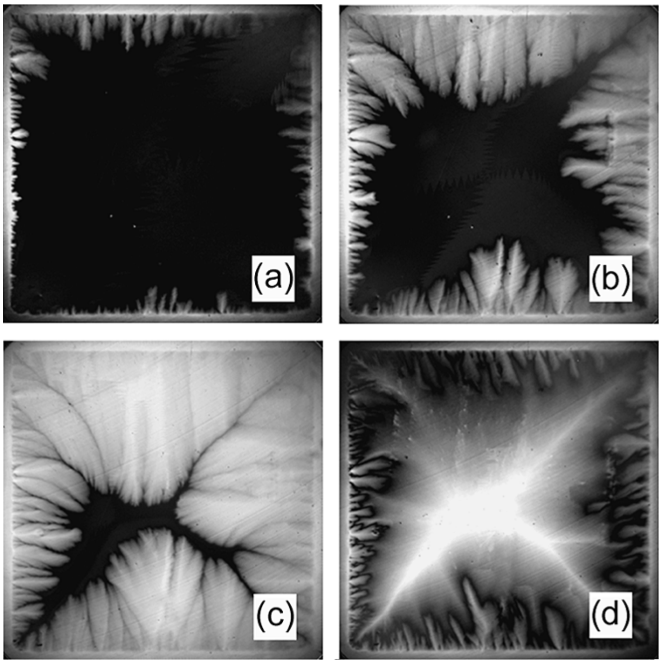

Fig. 1. Magneto-optical images of the ZFC ultra-pure $\mathrm{MgB_2}$ thin film ($5 \times 5\ \mathrm{mm^2}$) at $T = 4.2$ K. The perpendicular applied field $B_\mathrm{a} =$ (a) 10 mT, (b) 20 mT, (c) 40 mT, and (d) 0 (reduced from 0.1 T), respectively.

III. Results and Discussions

A. MOI of Ultra-Pure $\mathrm{MgB_2}$ Thin Films

Fig. 1 are the magneto-optical images showing regular flux penetration and trapping patterns in the zero-field-cooled (ZFC) ultra-pure $\mathrm{MgB_2}$ thin film ($5 \times 5\ \mathrm{mm^2}$) at $T = 4.2$ K during a perpendicular external field B_a increasing and decreasing cycle. When the local field at the sample edge was higher than the lower critical field H_{c1}, the magnetic flux started to penetrate gradually and uniformly into the sample from the edges. Fig. 1(a)–(c) are the images taken at $B_\mathrm{a} = 10$, 20, and 40 mT, respectively, showing regular penetration of the flux, consistent with critical state models. Correspondingly, when B_a was decreased, the flux exited the sample in the same manner. Fig. 1(d) shows a regular rooftop flux trapping pattern at the remnant state for the square film taken after B_a was reduced from 0.1 T to zero. The finger-like pattern is due to the roughness of the sample edge. The asymmetry of the flux pattern is perhaps due to the slight inhomogeneity of this $\mathrm{MgB_2}$ film. Similar flux penetration was observed at other temperatures except that the depth of penetration was different due to the temperature dependence of J_c. This phenomenon is in striking contrast to the earlier MOI studies of $\mathrm{MgB_2}$ thin films grown by PLD [2]–[4], where dendritic flux jumps were observed at $T < 10$ K.

B. Dentritic Flux Jump in Carbon-Doped $\mathrm{MgB_2}$ Thin Film

Fig. 2 shows dendritic flux penetration and exiting patterns in the ZFC carbon-doped $\mathrm{MgB_2}$ thin film ($5 \times 5\ \mathrm{mm^2}$) at $T = 4.2$ K during a field increasing and decreasing cycle. When the local field at the sample edge was larger than the lower critical field H_{c1}, the magnetic flux started to jump into the sample from the edges with a dendritic flux pattern. Fig. 2(a)–(d) are the images taken under perpendicular applied field $B_\mathrm{a} = 5, 7, 8$, and 15 mT, respectively, showing the dendritic flux jump. Once formed, the dendritic flux pattern seems frozen and new flux jumps happened at different positions on the edges. This phenomenon is completely different from the usual flux penetration described by critical state models. Correspondingly, flux exited the film in the same dendritic manner shown in Fig. 2(e) and (f), which were taken after B_a was reduced from 0.1 T to 8 mT and zero, respectively. Repeating the same procedure several times, we found that the flux jumps took place at random positions, indicating that this phenomenon is not the consequence of local defects. As the temperature increased, less dendritic flux jumps were observed. The dendritic flux jumps completely disappeared at temperatures higher than 10 K. This phenomenon is consistent with previous MOI studies of $\mathrm{MgB_2}$ thin films grown by PLD [2]–[4], where the dendritic flux jumps were abundant at $T < 10$ K.

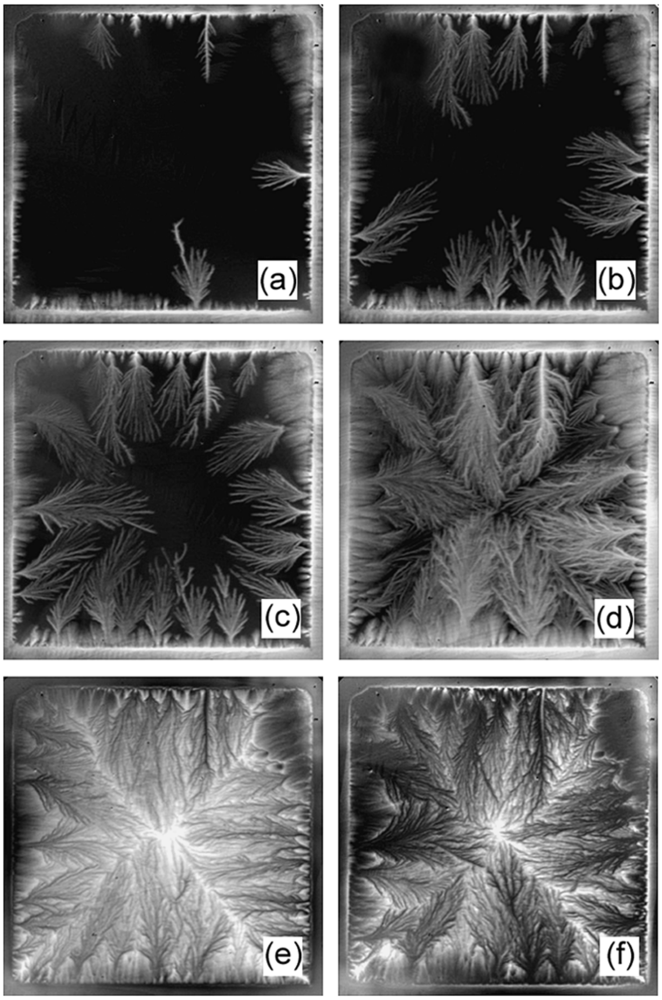

Fig. 2. Magneto-optical images of the ZFC carbon-doped $\mathrm{MgB_2}$ thin film ($5 \times 5\ \mathrm{mm^2}$) at $T = 4.2$ K showing the dendritic jump-in and exit of the magnetic flux. The perpendicular applied field $B_\mathrm{a} =$ (a) 5 mT, (b) 7 mT, (c) 8 mT, (d) 15 mT, (e) 8 mT (reduced from 0.1 T), and (f) 0 (reduced from 0.1 T), respectively.

C. Magnetization Measurements

Fig. 3 shows the results of the magnetization measurements of the ultra-pure and carbon-doped $\mathrm{MgB_2}$ thin films. Fig. 3(a)

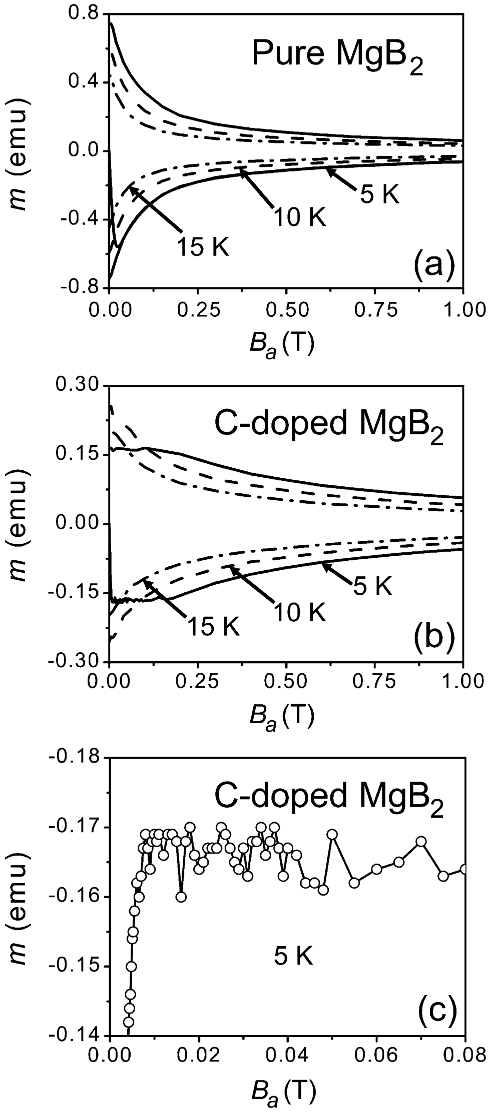

Fig. 3. Magnetization curves of the ultra-pure $\mathrm{MgB_2}$ thin film and the carbon-doped $\mathrm{MgB_2}$ thin film. (a) The hysteresis loop of the ultra-pure $\mathrm{MgB_2}$ thin film at $T = 5$, 10, and 15 K, respectively. (b) The hysteresis loops of the carbon-doped $\mathrm{MgB_2}$ thin film at the same temperatures. (c) The enlarged view of the magnetization curve for the carbon-doped film at 5 K.

is a part (B_{a} from 0 to 1 T) of the hysteresis loop (measured with B_{a} varying from -5 T to 5 T) for the ultra-pure $\mathrm{MgB_2}$ thin film at $T = 5$, 10, and 15 K, respectively, showing the regular critical state behaviors. The width of the loops Δm, defined as the difference of the magnetic moments with the same B_{a} on the increasing and descending branches of the loop, decreases as the temperature increases due to the lower J_{c} at higher temperatures. Fig. 3(b) is the hysteresis loop of the carbon-doped $\mathrm{MgB_2}$ thin film at the same field and temperature region, showing a suppressed low field magnetization at 5 K with a smaller Δm than those of higher temperatures due to the dendritic flux jumps. Fig. 3(c) is an enlarged view of the low field initial magnetization curve for the carbon-doped $\mathrm{MgB_2}$ thin film at 5 K, where dense oscillations are present. The J_{c} values evaluated from the magnetization hysteresis loops in Fig. 3 are comparable to those determined by transport measurements [9]–[11].

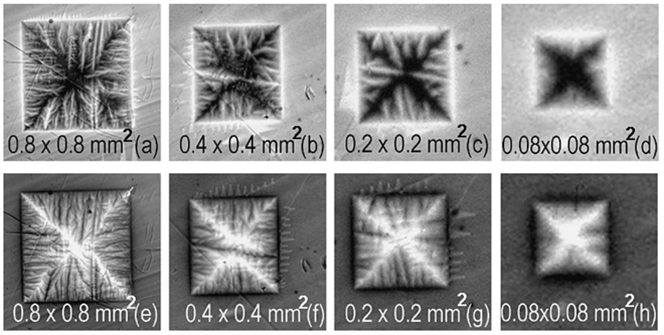

Fig. 4. Size-dependence of the dendritic flux patterns in carbon-doped $\mathrm{MgB_2}$ thin films. (a)–(d) were taken at $T = 4.2\ \mathrm{K}$ and $B_{\mathrm{a}} = 10\ \mathrm{mT}$ on samples of $0.8 \times 0.8\ \mathrm{mm}^2$, $0.4 \times 0.4\ \mathrm{mm}^2$, $0.2 \times 0.2\ \mathrm{mm}^2$, and $0.08 \times 0.08\ \mathrm{mm}^2$, respectively. (e)–(h) were taken at $T = 4.2\ \mathrm{K}$ and $B_{\mathrm{a}} = 10\ \mathrm{mT}$ reduced from 0.1 T.

D. Correlation Between Flux Jump and Materials Parameters

The combination of MOI studies, magnetization and transport measurements [9], [10] on the same series of $\mathrm{MgB_2}$ films gave us an opportunity to explore the correlation between flux jump and certain materials properties. The details of the analysis have been reported elsewhere [11]. To determine the key factors responsible for the disappearance of the dendritic flux jumps in the ultra-pure $\mathrm{MgB_2}$ films, we analyzed various parameters relevant to the thermo-magnetic instability. We found that the key parameter for the occurrence of the flux jump in $\mathrm{MgB_2}$ thin films is the flux flow resistivity $\rho_{\mathrm{f}} = \rho_{\mathrm{n}} B_{\mathrm{a}}/\mu_0 H_{\mathrm{c2}}$ [11]. ρ_{f} of the ultra-pure $\mathrm{MgB_2}$ films was more than one order of magnitude lower than the carbon-doped films.

E. Influence of Sample Size on the Dentritic Flux Jump Pattern in Carbon-Doped $\mathrm{MgB_2}$ *Films*

It is interesting to see how this dendritic flux pattern changes when the sample size is reduced. We trimmed the carbon-doped $\mathrm{MgB_2}$ thin film into a series of squares ranging from $0.8 \times 0.8\ \mathrm{mm}^2$ to $0.08 \times 0.08\ \mathrm{mm}^2$ in size. Fig. 4 shows the magneto-optical images of flux penetration and trapping patterns in these squares of superconducting $\mathrm{MgB_2}$ thin film. Fig. 4(a)–(d) are the magneto-optical images taken at $T = 4.2$ K and $B_{\mathrm{a}} = 10\ \mathrm{mT}$ during the initial flux penetration on the squares of $0.8 \times 0.8\ \mathrm{mm}^2$, $0.4 \times 0.4\ \mathrm{mm}^2$, $0.2 \times 0.2\ \mathrm{mm}^2$, and $0.08 \times 0.08\ \mathrm{mm}^2$, respectively. Fig. 4(e)–(h) were taken at $T = 4.2$ K and B_{a} reduced from 100 mT to 10 mT. It can be seen from these images that as the size is reduced, the flux pattern had fewer dendritic structures. Quantitative analysis about this sample-size-effect has been done and will be reported elsewhere.

IV. CONCLUSION

In conclusion, we have presented comparative MOI studies combined with magnetization measurements on an ultra-pure $\mathrm{MgB_2}$ film and a carbon-doped $\mathrm{MgB_2}$ film produced by HPCVD technique. In the ultra-pure $\mathrm{MgB_2}$ thin film, a regular magnetic flux penetration was observed, as predicted by the Bean critical state model. In the carbon-doped $\mathrm{MgB_2}$ thin film, dentritic flux jump was observed at low temperatures with low external magnetic field due to thermal magnetic instability, which was believed to be directly related to its high flux flow resistivity.

REFERENCES

[1] J. Nagamatsu, N. Nakagawa, T. Muranaka, Y. Zenitani, and J. Akimitsu, "Superconductivity at 39 K in magnesium diboride," *Nature*, vol. 410, pp. 63–64, Mar. 2001.

[2] T. H. Johansen, M. Baziljevich, D. V. Shantsev, P. E. Goa, Y. M. Galperin, W. N. Kang, H. J. Kim, E. M. Choi, M.-S. Kim, and S. I. Lee, "Dendritic magnetic instability in superconducting $\mathrm{MgB_2}$ films," *Europhys. Lett.*, vol. 59, pp. 599–605, Aug. 2002.

[3] M. Baziljevich, A. V. Bobyl, D. V. Shantsev, E. Altshuler, T. H. Johansen, and S. I. Lee, "Origin of dendritic flux patterns in $\mathrm{MgB_2}$ films," *Physica C*, vol. 369, pp. 93–96, Mar. 2002.

[4] Z. Ye, Q. Li, G. D. Gu, J. J. Tu, W. N. Kang, E.-M. Choi, H.-J. Kim, and S.-I. Lee, "Magneto-optical studies of the critical states in c-axis oriented $\mathrm{MgB_2}$ thin film and bulk $\mathrm{MgB_2/Mg}$ nano-composites," *IEEE Trans. Appl. Supercond.*, vol. 13, no. 2, pp. 3722–3725, Jun. 2003.

[5] Z. W. Zhao, S. L. Li, Y. M. Ni, H. P. Yang, Z. Y. Liu, H. H. Wen, W. N. Kang, H. J. Kim, E. M. Choi, and S. I. Lee, "Suppression of superconducting critical current density by small flux jumps in $\mathrm{MgB_2}$ thin films," *Phys. Rev. B*, vol. 65, p. 064 512, Jan. 2002.

[6] S. Jin, H. Mavoori, C. Bower, and R. B. van Dover, "High critical currents in iron-clad superconducting $\mathrm{MgB_2}$ wires," *Nature*, vol. 411, pp. 563–565, May 2001.

[7] S. X. Dou, X. L. Wang, J. Horvat, D. Milliken, A. H. Li, K. Konstantinov, E. W. Collings, M. D. Sumption, and H. K. Liu, "Flux jumping and a bulk-to-granular transition in the magnetization of a compacted and sintered $\mathrm{MgB_2}$ superconductor," *Physica C*, vol. 361, pp. 79–83, Sep. 2001.

[8] X. H. Zeng, A. V. Pogrebnyakov, A. Kotcharov, J. E. Jones, X. X. Xi, E. M. Lysczek, J. M. Redwing, S. Y. Xu, Q. Li, J. Lettieri, D. G. Schlom, W. Tian, X. Q. Pan, and Z. K. Liu, "In situ epitaxial $\mathrm{MgB_2}$ thin films for superconducting electronics," *Nature Materials*, vol. 1, pp. 35–38, Sep. 2002.

[9] S. Y. Xu, Q. Li, E. Wertz, Y. F. Hu, A. V. Pogrebnyakov, X. H. Zeng, X. X. Xi, and J. M. Redwing, "High critical current density and vortex pinning of epitaxial $\mathrm{MgB_2}$ thin films," *Phys. Rev. B*, vol. 68, p. 224 501, Dec. 2003.

[10] H.-J. Kim, W. N. Kang, E.-M. Choi, M.-S. Kim, K. H. P. Kim, and S.-I. Lee, "High current-carrying capability in c-axis-oriented superconducting $\mathrm{MgB_2}$ thin films," *Phys. Rev. Lett.*, vol. 87, p. 087 002, Aug. 2001.

[11] Z. Ye, Q. Li, Y. F. Hu, A. V. Pogrebnyakov, Y. Cui, X. X. Xi, J. M. Redwing, and Q. Li, "Electron scattering dependence of the dentritic magnetic instability in superconducting $\mathrm{MgB_2}$ films," *Appl. Phys. Lett.*, to be published.